Optical Hall conductivity in bulk and nanostructured graphene beyond the Dirac approximation

Jesper Goor Pedersen,[1] Mikkel H. Brynildsen,[2] Horia D. Cornean,[2] and Thomas Garm Pedersen[1,3]
[1]*Department of Physics and Nanotechnology, Aalborg University, Skjernvej 4A DK-9220 Aalborg East, Denmark*
[2]*Department of Mathematical Sciences, Aalborg University, Frederik Bajers Vej 7G, 9220 Aalborg East, Denmark*
[3]*Center for Nanostructured Graphene (CNG), Aalborg University, DK-9220 Aalborg East, Denmark*
(Received 10 July 2012; revised manuscript received 27 August 2012; published 26 December 2012)

We present a perturbative method for calculating the optical Hall conductivity in a tight-binding framework based on the Kubo formalism. The method involves diagonalization only of the Hamiltonian in absence of the magnetic field, and thus avoids the computational problems usually arising due to the huge magnetic unit cells required to maintain translational invariance in the presence of a Peierls phase. A recipe for applying the method to numerical calculations of the magneto-optical response is presented. We apply the formalism to the case of ordinary and gapped graphene in a next-nearest-neighbor tight-binding model as well as graphene antidot lattices. In both cases, we find unique signatures in the Hall response that are not captured in continuum (Dirac) approximations. These include a nonzero optical Hall conductivity even when the chemical potential is at the Dirac point energy. Numerical results suggest that this effect should be measurable in experiments.

DOI: 10.1103/PhysRevB.86.235438 PACS number(s): 81.05.ue, 78.20.Bh, 78.20.Ls

I. INTRODUCTION

Since the experimental discovery of graphene,[1] the honeycomb lattice has been the subject of intense research.[2–4] Graphene displays unique properties in an external magnetic field, with a nonequidistant Landau level structure and a zeroth Landau level energy which is independent of the magnetic field strength.[5–7] The Landau level structure is reflected in the half-integer quantum Hall effect observed in graphene,[8] which, due to graphene's large cyclotron gap, has been observed at room temperature.[9] These and other remarkable features of graphene emerge quite naturally from a low-energy, continuum description of graphene, the so-called Dirac approximation, which is based on a linearization of a nearest-neighbor (NN) tight-binding (TB) model near the high-symmetry K points.[10]

While many properties of graphene are correctly described by the Dirac model, it nevertheless fails in certain respects. A simple example is found in the optical response displaying a clear saddle point resonance around 4.4 eV that is absent in a linearized model.[11,12] More subtle effects such as an orbital magnetic susceptibility away from the Dirac point have been identified as consequences of lattice effects lost in a continuum approach.[13] Here, we demonstrate that under certain circumstances the Hall conductivity, which is routinely applied as an important tool to characterize graphene experimentally,[8,14,15] cannot be accurately described by the Dirac model. Specifically, the perfect electron-hole symmetry of the Dirac model, present also in the nonlinearized NN TB model, results in an optical Hall conductivity which is identically zero unless electron-hole symmetry is broken by moving the chemical potential away from the Dirac point energy.[16,17] In the present work, we predict that going beyond the Dirac model by including next-nearest-neighbor coupling in a full TB model yields an appreciable optical Hall response even when the chemical potential coincides with the Dirac point. This result is demonstrated using a perturbative technique that allows us to evaluate the magneto-optical response in an atomistic model for arbitrarily small field strengths. Thus, we identify a significant lattice effect, for which the Dirac model predicts a null result. We note that, interestingly, this deviation occurs for energies well within the range of the linearized band structure of graphene. It is thus not a result of simply probing the band structure beyond the validity of the linearized model, as is the saddle point resonance mentioned above, but is rather a strong signature of broken electron-hole symmetry.

To go beyond the Dirac model, we return to the tight-binding model from which the Dirac approximation emerges. The effect of a magnetic field can then be included via a Peierls substitution. The trouble with this method is that the periodicity of the Peierls phase, for realistic magnetic field strengths, is usually orders of magnitude larger than the lattice constant. Thus, calculations must be made on magnetic unit cells hundreds or thousands of times larger than the Wigner-Seitz cell. In the case of bulk materials, where the unit cell consists of just a few atoms, this problem may be overcome for large but reasonably realistic magnitudes of the magnetic field. However, for nanostructured graphene materials, where the Wigner-Seitz cell may itself contain hundreds of atoms, direct diagonalization of the resulting Hamiltonian is not feasible. Several numerical methods have previously been suggested to overcome this problem.[18–20] However, all these methods eventually fail at sufficiently small magnetic fields, because of the divergence of the size of the magnetic unit cell.

In this paper, we present a perturbative approach to calculating the optical Hall conductivity in TB models on a honeycomb lattice. The approach requires diagonalization only of the Hamiltonian in the *absence* of the magnetic field, and thus circumvents the problem associated with the periodicity of the Peierls phase. We apply the formalism first to ordinary and gapped graphene, illustrating clear and qualitative deviations from a Dirac approximation, as discussed above. Finally, to illustrate the power of the perturbative formalism, we apply the method to an example of nanostructured graphene, in this case graphene antidot lattices,[21,22] and once again find qualitative differences in the optical Hall conductivity compared to a simple continuum treatment.

II. PERTURBATIVE METHOD

The derivation of the main result of the perturbative treatment is given in full details in Ref. 23. The approach is based on the strategy developed in Refs. 24 and 25. The starting point is a TB approximation of the honeycomb lattice without magnetic field. The optical conductivity is then evaluated using the Kubo formalism, with the effect of the magnetic field included perturbatively via a Peierls substitution. That is, a phase is added to the hopping terms t_{ij} between atomic sites i and j, such that $t_{ij} \to t_{ij}e^{i\phi}$, with the phase given as $\phi = e/\hbar \times \int_{\mathbf{R_i}}^{\mathbf{R_j}} \mathbf{A}\cdot d\mathbf{l}$. Here, $\mathbf{R_i}$ and $\mathbf{R_j}$ denote the positions of the atomic sites, while $\mathbf{A}$ is the magnetic vector potential. Including the effect of the magnetic field to first order, the result for the optical Hall conductivity reads as

$$\sigma_{xy}(\omega) = \frac{Be^3}{16\pi^3\hbar^3\omega}\int d\mathbf{k}\mathrm{Re}\oint_{\mathcal{C}} dz \times \{if(z)\mathrm{Tr}[T_{xy}(z) + T_{xy}(z+\hbar\omega)]\}. \quad (1)$$

Also, we note that all even powers of the expansion in the magnetic field strength are zero, so the equation is valid up to third order in the magnetic field strength. Here, B is the magnetic field strength, e is the electron charge, $\hbar\omega$ is the photon energy, and $f(z)$ is the Fermi-Dirac distribution function. The first integral is over the Brillouin zone, while the last integral is to be taken along a contour $\mathcal{C}$, which should enclose the entire energy spectrum of the Hamiltonian H, while $\mathcal{C} \pm \hbar\omega$ should not contain the spectrum. Here, and in what follows, we include a small imaginary part in $\hbar\omega = \hbar\omega_0 + i\hbar\Gamma$ to account for broadening. Note that a spin degeneracy factor has not been included, and the final trace thus includes tracing over spin degrees of freedom. This trace is over the operators $T_{xy}(z) \equiv T^{(1)}_{xy}(z) + T^{(2)}_{xy}(z)$, with

$$T^{(1)}_{xy}(z) \equiv \{\tilde{G}_y H_y G_x - \tilde{G}_x H_y G_y + \tilde{G}[H_y G(H_y G_x - H_x G_y) + (H_y\tilde{G}_x - H_x\tilde{G}_y)H_y G]\}H_x \quad (2)$$

and

$$T^{(2)}_{xy}(z) \equiv [(\tilde{G}_y H_{xy} - \tilde{G}_x H_{yy})G + \tilde{G}(H_{yy}G_x - H_{xy}G_y)]H_x. \quad (3)$$

Here, we have defined the derivatives of the Hamiltonian $H_i \equiv \partial H/\partial k_i$ and $H_{ij} \equiv \partial^2 H/\partial k_i \partial k_j$, with similar definitions for the Green's functions $G = (H - z)^{-1}$ and $\tilde{G} = (H - z + \hbar\omega)^{-1}$. We stress that because the magnetic field is treated as a perturbation, the Hamiltonian appearing in these expressions is the Hamiltonian in *absence* of the magnetic field. For numerical calculations, this is a significant advantage of this method, as we will demonstrate in more detail below.

III. LINEARIZED GRAPHENE

Before turning to the full TB model, we wish to apply the above approach to demonstrate that, indeed, the Hall conductivity in the linearized model vanishes if electron-hole symmetry remains unbroken. We consider the TB Hamiltonian corresponding to the unit cell of graphene shown in Fig. 1(a). For generality, in addition to ordinary bulk graphene, we consider also a gapped graphene model, where a staggered mass term $\pm\Delta$ is added to the on-site energies, with the sign

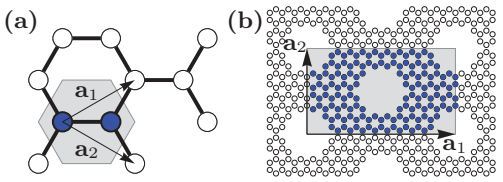

FIG. 1. (Color online) Unit cells used for the analytical and numerical calculations of the optical Hall conductivity of (a) bulk graphene and (b) a {4,2} graphene antidot lattice. The gray shading indicates the size of the unit cell, with highlighted carbon atoms included in the unit cell. Note that the rectangular unit cell for the GAL is chosen for computational convenience only.

alternating between the two sublattices of graphene. Pristine graphene may exhibit a gap due to excitonic effects.[26,27] However, here we will focus on magnitudes of the gap that are relevant for nanoengineered graphene, such as graphene antidot lattices.[21,22] We stress that the results obtained remain qualitatively the same for any magnitude of the gap. Linearized around the K point, we find that the optical Hall conductivity can be evaluated as

$$\frac{\sigma_{xy}(\omega)}{\sigma_0} = \frac{4\omega_c^2}{\pi\omega^2}\int_{\Delta}^{\infty} d\epsilon \frac{\hbar^2\omega^2 + 2\Delta^2 - 2\epsilon^2}{\hbar^2\omega^2 - 4\epsilon^2}[f'(-\epsilon) - f'(\epsilon)], \quad (4)$$

where we have introduced the zero-frequency graphene conductivity $\sigma_0 \equiv e^2/4\hbar$ and the cyclotron frequency $\omega_c \equiv v_F\sqrt{2eB/\hbar}$, with v_F the Fermi velocity. We note that the K and K' valleys contribute equally, and that a factor of 2 to account for this valley degeneracy has already been included in the above equation. This result agrees with the low field strength limit of previous analytical results derived by Gusynin *et al.*[28] The full details of the derivation of Eq. (4) are given in the Appendix. We note that the final term $f'(-\epsilon) - f'(\epsilon) \propto \sinh(\mu/kT)$ with μ the chemical potential while kT is the thermal energy. This demonstrates how the optical Hall conductivity is identically zero in the symmetrical case, where the chemical potential sits at the Dirac point energy. Below, we will demonstrate how this zero result is drastically altered when going beyond the continuum (Dirac) treatment of graphene.

IV. NUMERICAL RESULTS

The analytical result for linearized graphene, presented above, is interesting in its own right, and serves as a way of validating the perturbative approach. However, the real power of the method lies in the fact that because the expression in Eq. (1) is given in terms of the Hamiltonian *without* magnetic field, numerical TB calculations can be performed on a drastically smaller unit cell than using the standard method of Peierls substitution in a nonperturbative manner. Peierls substitution necessitates a magnetic unit cell large enough to ensure periodicity of the magnetic phase factor added to the hopping terms. For graphene, this leads to a scaling of the total number of carbon atoms as $N \simeq 316 \times 10^3\,\mathrm{T} \times B^{-1}$, rendering realistic magnetic fields quite difficult to manage using this method.[17]

A. Numerical recipe

To arrive at an expression suitable for numerical simulations, we first note the identity $G_i = -GH_iG$, with $H_i \equiv \partial H/\partial k_i$, and a similar definition for the Green's functions $G = (H - z)^{-1}$ and $\tilde{G} = (H - z + \hbar\omega)^{-1}$. Using this identity we write the trace in the eigenstate basis as

$$\mathrm{Tr}\left[T^{(1)}_{xy}(z)\right] = \sum_{mnpq}\left\{\frac{M^{xxyy}_{mnpq} - M^{yxxy}_{mnpq}}{(E_m - z_-)(E_n - z_-)(E_p - z)(E_q - z)} + \frac{M^{xyxy}_{mnpq} - M^{xxyy}_{mnpq}}{(E_m - z_-)(E_n - z)(E_p - z)(E_q - z)} + \frac{M^{yxxy}_{mnpq} - M^{xyxy}_{mnpq}}{(E_m - z_-)(E_n - z_-)(E_p - z_-)(E_q - z)}\right\}, \tag{5}$$

where we have introduced $z_\pm = z \pm \hbar\omega$ and

$$M^{ijkl}_{mnpq} = \langle m|H_i|n\rangle\langle n|H_j|p\rangle\langle p|H_k|q\rangle\langle q|H_l|m\rangle. \tag{6}$$

We can now perform the contour integration using the residue theorem. To ease notation we define $E_{mn} = E_m - E_n$ and $M^{ijkl,i'j'k'l'}_{mnpq} = M^{ijkl}_{mnpq} - M^{i'j'k'l'}_{mnpq}$, as well as $\bar{\delta}_{mn} = 1 - \delta_{mn}$ and $\bar{\delta}_{mnp} = \bar{\delta}_{mn}\bar{\delta}_{np}\bar{\delta}_{pm}$, where δ_{mn} is the Kronecker delta. We then arrive at the rather lengthy expression

$$\begin{aligned}\oint_{\mathcal{C}} f(z)\mathrm{Tr}\left[T^{(1)}_{xy}(z)\right]dz = 2\pi i \sum_{mnpq}\Bigg\{&\bar{\delta}_{pq}\frac{M^{xxyy,yxxy}_{mnpq}}{E_{pq}}\left(\frac{f(E_p)}{(E_{mp}+\Omega)(E_{np}+\Omega)} - \frac{f(E_q)}{(E_{mq}+\Omega)(E_{nq}+\Omega)}\right)\\ &+\delta_{pq}M^{xxyy,yxxy}_{mnpp}\frac{(E_{mp}+E_{np}+2\Omega)f(E_p)+(E_{mp}+\Omega)(E_{np}+\Omega)f'(E_p)}{(E_{mp}+\Omega)^2(E_{np}+\Omega)^2}\\ &+\bar{\delta}_{npq}\left(M^{xyxy,xxyy}_{mnpq}+M^{xyxy,xxyy}_{mpnq}+M^{xyxy,xxyy}_{mpqn}\right)\frac{f(E_n)}{E_{np}E_{nq}(E_{nm}-\Omega)}\\ &+\delta_{np}\bar{\delta}_{nq}\frac{M^{xyxy,xxyy}_{mnnq}+M^{xyxy,xxyy}_{mnqn}+M^{xyxy,xxyy}_{mqnn}}{E^2_{nq}}\\ &\times\left(\frac{(E_{mn}+E_{qn}+\Omega)f(E_n)+E_{qn}(E_{mn}+\Omega)f'(E_n)}{(E_{mn}+\Omega)^2}+\frac{f(E_q)}{E_{qm}-\Omega}\right)\\ &-\delta_{nq}\delta_{pq}M^{xyxy,xxyy}_{mnnn}\frac{(E_{mn}+\Omega)\,f'(E_n)+\frac{1}{2}(E_{mn}+\Omega)^2\,f''(E_n)+f(E_n)}{(E_{mn}+\Omega)^3}\\ &-\frac{M^{yxxy,xyxy}_{mnpq}f(E_q)}{(E_{mq}+\Omega)(E_{nq}+\Omega)(E_{pq}+\Omega)}\Bigg\},\end{aligned} \tag{7}$$

where we have introduced $\Omega = \hbar\omega$. In a similar fashion, we write the trace over the second operator as

$$\mathrm{Tr}\left[T^{(2)}_{xy}(z)\right] = \sum_{mnp}\left\{\frac{N^{yxyx}_{pmn} - N^{yxxy}_{pmn}}{(E_m - z_-)(E_n - z)(E_p - z)} - \frac{N^{xxyy}_{mnp} - N^{yxxy}_{mnp}}{(E_m - z_-)(E_n - z_-)(E_p - z)}\right\}, \tag{8}$$

where we have defined

$$N^{ijkl}_{mnp} = \langle m|H_i|n\rangle\langle n|H_{jk}|p\rangle\langle p|H_l|m\rangle. \tag{9}$$

The residue theorem then leads to

$$\begin{aligned}\oint_{\mathcal{C}} f(z)\mathrm{Tr}\left[T^{(2)}_{xy}(z)\right]dz = 2\pi i\sum_{mnp}\Bigg\{&N^{xxyy,yxxy}_{mnp}\frac{f(E_p)}{(E_{mp}+\Omega)(E_{np}+\Omega)} + \bar{\delta}_{np}\frac{N^{yxyx,yxxy}_{pmn}}{E_{np}}\left(\frac{f(E_n)}{E_{mn}+\Omega} - \frac{f(E_p)}{E_{mp}+\Omega}\right)\\ &+\delta_{np}N^{yxyx,yxxy}_{nmn}\frac{f(E_n)+(E_{mn}+\Omega)\,f'(E_n)}{(E_{mn}+\Omega)^2}\Bigg\}.\end{aligned} \tag{10}$$

The trace of the operators with the shifted argument is obtained in a similar fashion. By substituting $z \to z_+$ and $z_- \to z$ in Eq. (5) and relabeling slightly, one can show that the contour integral $\oint_{\mathcal{C}} f(z)\mathrm{Tr}[T^{(1)}_{xy}(z+\Omega)]$ is given by Eq. (7), if one substitutes

$$\Omega \to -\Omega, \quad M^{xxyy,yxxy}_{mnpq} \to M^{xxyy,yxxy}_{qpnm}, \quad M^{yxxy,xyxy}_{mnpq} \to M^{xyxy,xxyy}_{qpnm}, \quad M^{xyxy,xxyy}_{mnpq} \to M^{yxxy,xyxy}_{qpnm}. \tag{11}$$

Similarly, $\oint_{\mathcal{C}} f(z)\mathrm{Tr}[T^{(2)}_{xy}(z+\Omega)]$ is given by Eq. (10), with the substitutions

$$\Omega \to -\Omega, \quad N^{xxyy,yxxy}_{nmp} \to N^{yxxy,yxyx}_{mpn}, \quad N^{yxyx,yxxy}_{pnm} \to N^{yxxy,xxyy}_{pnm}. \tag{12}$$

In this way we have arrived at expressions for the contour integral of the trace in Eq. (1) in terms of sums over the eigenstates of the Hamiltonian without magnetic field. These sums can be truncated to include only states near the Fermi energy. For small magnetic fields, this method is drastically faster than direct diagonalization of the Hamiltonian with magnetic field, the size of which diverges as the magnetic field strength is reduced. In all numerical results presented below, we set the thermal energy to $kT = 0.025$ eV and include a broadening of $\hbar\Gamma = 0.05$ eV.

B. Graphene

We now consider a next-nearest-neighbor (NNN) TB model of gapped graphene, defined via the Hamiltonian

$$H(\mathbf{k}) = \begin{bmatrix} t'g(\mathbf{k}) + \Delta & -tf(\mathbf{k}) \\ -tf^*(\mathbf{k}) & t'g(\mathbf{k}) - \Delta \end{bmatrix}, \tag{13}$$

parametrized by the nearest- and next-nearest-neighbor hopping parameters $t = 3$ eV and $t' = 0.3$ eV, respectively. Here, $f(\mathbf{k}) = e^{ik_x a_c} + 2e^{-ik_x a_c/2}\cos(\sqrt{3}k_y a_c/2)$, while $g(\mathbf{k}) = 2\cos(\sqrt{3}k_y a_c) + 4\cos(3k_x a_c/2)\cos(\sqrt{3}k_y a_c/2)$, where $a_c = a/\sqrt{3}$ is the carbon-carbon distance. While the hopping parameters can vary slightly depending on which *ab initio* results they are fitted to, we note that the exact value of the hopping terms do not alter our results qualitatively. We set the on-site energy to zero. For $t' = 0$, this model has electron-hole symmetry, which is inherited in the Dirac model discussed above. We note that linearization of any TB model will inevitably result in perfect electron-hole symmetry. As discussed above, in the fully symmetrical situation, where the chemical potential sits at the Dirac point energy, the off-diagonal conductivity is identically zero for any such model. This can be proven on quite general terms for all TB models exhibiting π-π^* symmetry, for which contributions from conjugate transitions exactly cancel in the fully symmetrical case.[16,17] Introducing next-nearest-neighbor coupling breaks electron-hole symmetry and, as we will now demonstrate, leads to a markedly different magneto-optical response of graphene.

In Fig. 2 we show the calculated optical Hall conductivity of graphene, with the chemical potential at the Dirac point energy. While the Dirac approximation (and nearest-neighbor TB) predicts a zero response in this case, our NNN TB model suggests a clear resonance at $\hbar\omega = 2\Delta$. This drastic deviation from the Dirac model is due to the broken electron-hole symmetry, which means that conjugate transitions in the optical response no longer cancel entirely.[17] The strength of the resonance decreases as the magnitude of the band gap is increased, in agreement with previous results showing that a sufficiently large band gap effectively quenches the effect of the magnetic field, provided $\Delta \gg \hbar\omega_c$.[17] However, the magnitude of this correction to the Dirac response is quite appreciable, suggesting that these deviations from the Dirac model should be measurable in experiments. We note that, as expected, numerical calculations show similar results for a nearest-neighbor model if overlap between neighboring π orbitals is included.

For comparison with the perturbative results, we also show the Hall conductivity for $\Delta = 0.1$ eV and a magnetic field strength of $B = 26.3$ T, calculated using standard, nonperturbative tight-binding methods.[17] We note that these calculations involve a Hamiltonian with 12000×12000 elements for what is a quite strong magnetic field. The relationship with the perturbative result is evident in the figure, and illustrates the fact that the perturbative results still have predictive power for the strength of the response even in substantial magnetic fields. In particular, the perturbative results correspond to an averaging of the oscillations occurring due to individual Landau levels, which for smaller magnetic field strengths could presumably be caused by a broadening of the order of the cyclotron energy.

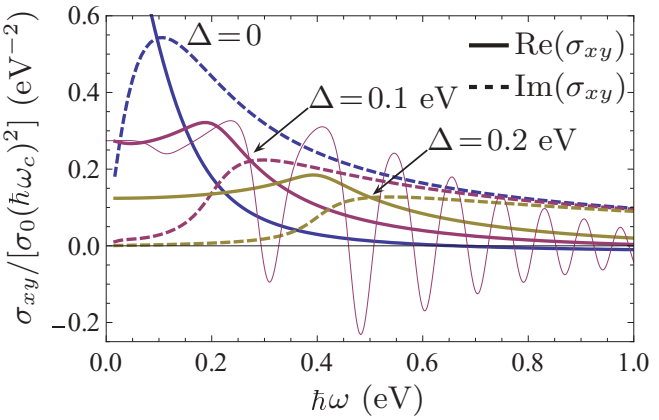

FIG. 2. (Color online) Optical Hall conductivity σ_{xy} as a function of photon energy for ordinary graphene and gapped graphene with increasing values of the mass term. The chemical potential is in the middle of the gap. The conductivity is shown relative to the zero-frequency conductivity of graphene σ_0 times the square of the cyclotron energy $\hbar\omega_c$. The solid (dashed) lines show the real (imaginary) part of the conductivity. To ease visibility, the response of ordinary graphene has been cropped. The DC value of ordinary graphene is $\sigma_{xy}(0) \simeq (\hbar\omega_c)^2\sigma_0 \times 1.03$ eV^{-2}. The thin line shows the real part of the Hall conductivity for $\Delta = 0.1$ eV and a magnetic field of $B = 26.3$ T.

To further corroborate these findings, we will now derive an approximate, semianalytical expression for the optical Hall conductivity in the next-nearest-neighbor model. We first note that linearizing the NNN Hamiltonian in Eq. (13) near the K point yields the same result as the nearest-neighbor model, except for a constant diagonal term. Instead, we proceed by expanding the diagonal NNN term to second order near the K point, yielding the approximate Hamiltonian

$$H(\mathbf{k}) \simeq \begin{bmatrix} \frac{9}{8}\tau\kappa^2 + \Delta & \frac{3}{2}(\kappa_x - i\kappa_y) \\ \frac{3}{2}(\kappa_x + i\kappa_y) & \frac{9}{8}\tau\kappa^2 - \Delta \end{bmatrix}, \tag{14}$$

where we have defined $\kappa_i = tk_i a_c$ and introduced the parameter $\tau = 2t'/t^2$, quantifying the perturbation due to NNN coupling. The eigenvalues of this Hamiltonian read $E_\pm = \frac{9}{8}\tau\kappa^2 \pm \sqrt{\Delta^2 + \frac{9}{4}\kappa^2}$. We now proceed in a manner similar to that of the Appendix; i.e., we evaluate the trace of $T_{xy}(z)$, integrate out the angular component of the Brillouin zone integral, and then use the residue theorem to perform the contour integral over z in Eq. (1). In this manner, we find that the optical Hall conductivity in the NNN model is approximately

given by

$$\sigma_{xy}(\omega) = \sigma_0 \frac{4\omega_c^2}{\pi\omega^2} \int_\Delta^\infty \frac{\frac{1}{2}\tau(3\epsilon^2 - \Delta^2)\hbar^2\omega^2 [f(E_+) - f(E_-)] + a_-(\epsilon) f'(E_-) + a_+(\epsilon) f'(E_+)}{\epsilon^2(\hbar^2\omega^2 - 4\epsilon^2)} \, d\epsilon, \tag{15}$$

where we have introduced

$$a_\pm(\epsilon) = \epsilon\{2\epsilon(\tau\epsilon \pm 1)(1 - (\tau\epsilon)^2)(\epsilon^2 - \Delta^2) - \hbar^2\omega^2(\pm\epsilon - \tfrac{1}{2}\tau[(\tau\epsilon)^2 - 1 \pm 2\tau\epsilon](\epsilon^2 - \Delta^2))\}, \tag{16}$$

where $E_\pm = \frac{1}{2}\tau(\epsilon^2 - \Delta^2) \pm \epsilon$, with $\epsilon = \sqrt{\Delta^2 + \frac{9}{4}\kappa^2}$. In Fig. 3 we compare the numerical results with those obtained by numerical integration of the analytical result derived above. We note that there is excellent agreement between the two methods.

C. Graphene antidot lattices

Nanostructured graphene systems, with Wigner-Seitz unit cells containing on the order of hundreds of atoms, are practically impossible to handle using direct diagonalization of the TB Hamiltonian in the presence of a realistic magnetic field. To illustrate the power of the perturbative method presented above, we now consider the magneto-optical response of periodically perforated graphene, so-called graphene antidot lattices (GALs).[21] The low-energy spectrum of these structures can be quite accurately described in a gapped graphene model, by fitting the mass term to coincide with half the magnitude of the GAL band gap.[29] We now compare TB results to such a continuum description of GALs. For these results we ignore next-nearest-neighbor coupling, to illustrate how deviations from a continuum approximation emerge even in the simplest nearest-neighbor TB treatment. We denote a given GAL structure as $\{L,R\}$, where L is the side length of the hexagonal Wigner-Seitz cell, while R denotes the radius of the circular hole in the middle of the cell, both in units of the graphene lattice constant. We consider a geometry for which the superlattice basis vectors are parallel to the carbon-carbon bonds, as such structures always exhibit band gaps.[30] As an example, Fig. 1(b) shows the computational cell of a {4,2} GAL, highlighted with gray shading. We note that the rectangular unit cell contains 144 carbon atoms. For comparison, a standard nonperturbative calculation of the magneto-optical properties would require a magnetic unit cell consisting of 72000 carbon atoms, even for a substantial magnetic field strength of 40 T.

In Fig. 4 we show the optical Hall conductivity of the {4,2} GAL calculated using the perturbative approach. For comparison we also show the corresponding result for gapped graphene, with a mass term equal to half the band gap of the GAL, $\Delta \simeq 0.58$ eV. In both cases, we fix the chemical potential at the lower band gap edge; i.e., $\mu = \Delta$. We find reasonable agreement between the full GAL calculations and the simpler gapped graphene model. However, we note that a distinct feature of the GAL structure is the additional resonance near $\hbar\omega = 1.65$ eV, which is absent in the simpler gapped graphene Dirac model. This resonance occurs due to transitions between bands that are not present in a simple two-band gapped graphene model of GALs. We will explore the details of the magneto-optical response of graphene antidot lattices in future work, and include the result here mainly to emphasize the power of the perturbative formalism presented.

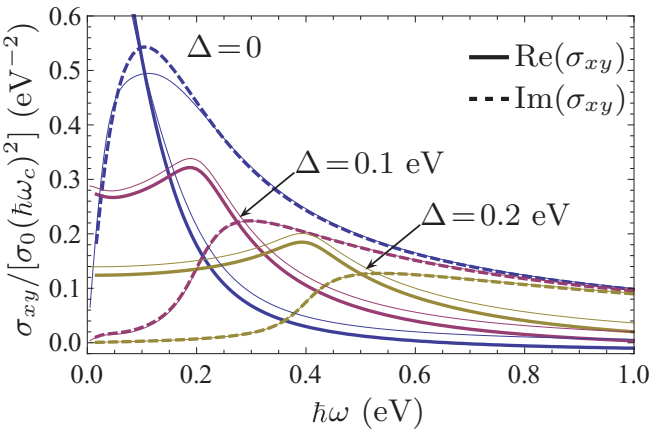

FIG. 3. (Color online) Optical Hall conductivity σ_{xy} as a function of photon energy for ordinary graphene and gapped graphene with increasing values of the mass term. The chemical potential is in the middle of the gap. The conductivity is shown relative to the zero-frequency conductivity of graphene σ_0 times the square of the cyclotron energy $\hbar\omega_c$. The solid (dashed) lines show the real (imaginary) part of the conductivity. The thin lines show the corresponding results obtained via the semianalytical expression derived in the main text.

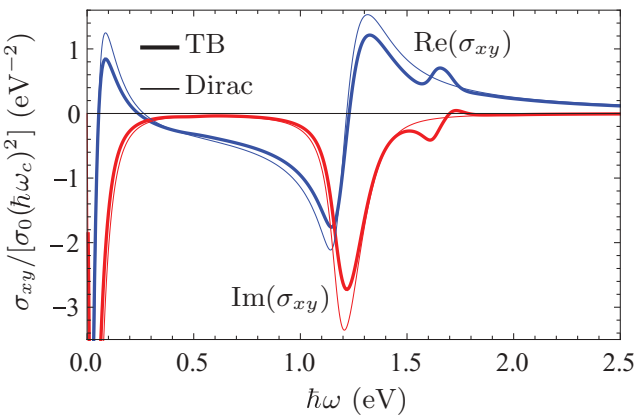

FIG. 4. (Color online) Optical Hall conductivity σ_{xy} as a function of photon energy for the {4,2} graphene antidot lattice. The conductivity is shown relative to the zero-frequency conductivity of graphene σ_0 times the square of the cyclotron energy $\hbar\omega_c$. The blue (red) lines show the real (imaginary) part of the conductivity. The thick lines show the results of the perturbative method applied to the GAL structure, while the thin lines are results of a gapped graphene Dirac model with a band gap corresponding to the GAL.

V. SUMMARY

A perturbative approach to calculating the optical Hall conductivity of graphene structures has been presented and applied to tight-binding models of graphene and graphene antidot lattices. The optical Hall response of graphene shows significant deviations from a simple Dirac treatment. While the Dirac model predicts a Hall conductivity of identically zero for a chemical potential at the Dirac point energy, results from our next-nearest neighbor tight-binding model indicate clear resonances at the band gap. The numerical results suggest that these effects should be measurable in experiments. Results for graphene antidot lattices illustrate that in this case, even the simple nearest-neighbor tight-binding model gives qualitatively different results than a simple Dirac approximation.

ACKNOWLEDGMENTS

The work by J.G.P. is financially supported by the Danish Council for Independent Research, FTP Grants No. 11-105204 and No. 11-120941. The Center for Nanostructured Graphene (CNG) is sponsored by the Danish National Research Foundation.

APPENDIX: LINEARIZED GRAPHENE

Linearizing the tight-binding Hamiltonian of gapped graphene near the K point results in the celebrated Dirac approximation of graphene,

$$H = \begin{bmatrix} \Delta & \frac{3}{2}(\kappa_x - i\kappa_y) \\ \frac{3}{2}(\kappa_x + i\kappa_y) & -\Delta \end{bmatrix}, \tag{A1}$$

where we have introduced $\kappa_i = tk_i a_c$, with a_c the nearest-neighbor distance $a_c = a/\sqrt{3}$. We use this form of the Hamiltonian to evaluate the trace, noting that the linearization means that $T^{(2)}_{xy} = 0$. In polar coordinates $(\kappa_x, \kappa_y) = \kappa(\cos\phi, \sin\phi)$ we find, after integrating over the angular component,

$$\int d\phi\ \mathrm{Tr}[T_{xy}(z)] = \frac{10368\pi t^4 a_c^4 \Omega(\Omega - 2z)[z(\Omega - z) + \Delta^2]}{[9\kappa^2 - 4((\Omega - z)^2 - \Delta^2)]^2[9\kappa^2 - 4(z^2 - \Delta^2)]^2}, \tag{A2}$$

where $\Omega = \hbar\omega$ is the photon energy. We now use the residue theorem to perform the contour integral over z, yielding

$$\oint_C dz\ if(z) \int d\phi\ \mathrm{Tr}[T_{xy}(z) + T_{xy}(z + \Omega)] = \frac{81\pi^2 t^4 a_c^4 (9\kappa^2 - 2\Omega^2)}{2\Omega\sqrt{9\kappa^2 + 4\Delta^2}(9\kappa^2 + 4\Delta^2 - \Omega^2)} \times [f'(-\sqrt{9\kappa^2/4 + \Delta^2}) - f'(\sqrt{9\kappa^2/4 + \Delta^2})], \tag{A3}$$

where poles at $z = 2\Omega \pm \sqrt{9\kappa^2/4 + \Delta^2} = 2\Omega \pm \epsilon(k)$ have been ignored because, as discussed in the paper, the contour explicitly excludes these points. Inserting this result in Eq. (1) of the paper and converting the Brillouin zone integration to an integral over energy, this leads to Eq. (4) of the main text. Taking as their starting point the Landau level structure of gapped graphene, Gusynin *et al.* have previously derived the off-diagonal magneto-optical conductivity of gapped graphene.[28] Their result is stated as a sum over Landau levels,

$$\frac{\sigma_{xy}(\omega)}{\sigma_0} = \frac{2\hbar^2\omega_c^2}{\pi} \sum_{n=0}^{\infty} ([f(-\epsilon_{n+1}) - f(-\epsilon_n)] - [f(\epsilon_n) - f(\epsilon_{n+1})]) \times \left[\left(1 - \frac{\Delta^2}{\epsilon_n \epsilon_{n+1}}\right) \frac{1}{(\epsilon_{n+1} - \epsilon_n)^2 - \Omega^2} + \left(1 + \frac{\Delta^2}{\epsilon_n \epsilon_{n+1}}\right) \frac{1}{(\epsilon_{n+1} + \epsilon_n)^2 - \Omega^2} \right], \tag{A4}$$

where the energies are $\epsilon_n = \sqrt{\Delta^2 + n\hbar^2\omega_c^2}$ for $n \geqslant 0$, yielding $\epsilon_{n+1} = \epsilon_n\sqrt{1 + \hbar^2\omega_c^2/\epsilon_n^2} \simeq \epsilon_n + \hbar^2\omega_c^2/(2\epsilon_n)$ in the low-field limit. Thus, in the continuum limit $\frac{d\epsilon}{dn} = \hbar^2\omega_c^2/2$. Replacing $f(\epsilon_n) - f(\epsilon_{n+1}) \to -f'(\epsilon_n)\frac{d\epsilon}{dn}$ and converting the sum to an integral via $\sum_n \frac{d\epsilon}{dn} \to \int d\epsilon$, we recover Eq. (4).

[1] K. S. Novoselov, A. K. Geim, S. V. Morozov, D. Jiang, Y. Zhang, S. V. Dubonos, I. V. Grigorieva, and A. A. Firsov, Science **306**, 666 (2004).
[2] A. K. Geim and K. S. Novoselov, Nat. Mater. **6**, 183 (2007).
[3] A. K. Geim, Science **19**, 1530 (2009).
[4] A. H. Castro Neto, F. Guinea, N. M. R. Peres, K. S. Novoselov, and A. K. Geim, Rev. Mod. Phys. **81**, 109 (2009).
[5] K. S. Novoselov, A. K. Geim, S. V. Morozov, D. Jiang, M. I. Katsnelson, I. V. Grigorieva, S. V. Dubonos, and A. A. Firsov, Nature (London) **438**, 197 (2005).
[6] V. P. Gusynin and S. G. Sharapov, Phys. Rev. Lett. **95**, 146801 (2005).
[7] V. P. Gusynin and S. G. Sharapov, Phys. Rev. B **71**, 125124 (2005).
[8] Y. Zhang, Y.-W. Tan, H. L. Stormer, and P. Kim, Nature (London) **438**, 201 (2005).
[9] K. S. Novoselov, Z. Jiang, Y. Zhang, S. V. Morozov, H. L. Stormer, U. Zeitler, J. C. Maan, G. S. Boebinger, P. Kim, and A. K. Geim, Science **315**, 1379 (2007).
[10] G. W. Semenoff, Phys. Rev. Lett. **53**, 2449 (1984).
[11] T. G. Pedersen, Phys. Rev. B **67**, 113106 (2003).
[12] V. G. Kravets, A. N. Grigorenko, R. R. Nair, P. Blake, S. Anissimova, K. S. Novoselov, and A. K. Geim, Phys. Rev. B **81**, 155413 (2010).
[13] G. Gómez-Santos and T. Stauber, Phys. Rev. Lett. **106**, 045504 (2011).
[14] K. S. Kim *et al.*, Nature (London) **457**, 706 (2009).
[15] K. I. Bolotin *et al.*, Solid State Commun. **146**, 351 (2008).
[16] T. G. Pedersen, Phys. Rev. B **68**, 245104 (2003).
[17] J. G. Pedersen and T. G. Pedersen, Phys. Rev. B **84**, 115424 (2011).
[18] R. Haydock, J. Phys. C **5**, 2845 (1972).

[19]G. Czycholl and W. Ponischowski, Z. Phys. B **73**, 343 (1988).
[20]R. B. S. Oakeshott and A. MacKinnon, J. Phys.: Condens. Matter **5**, 6971 (1993).
[21]T. G. Pedersen, C. Flindt, J. Pedersen, N. A. Mortensen, A.-P. Jauho, and K. Pedersen, Phys. Rev. Lett. **100**, 136804 (2008).
[22]J. A. Fürst, J. G. Pedersen, C. Flindt, N. A. Mortensen, M. Brandbyge, T. G. Pedersen, and A.-P. Jauho, New J. Phys. **11**, 095020 (2009).
[23]M. H. Brynildsen and H. D. Cornean, arXiv:1112.2613.
[24]H. D. Cornean, G. Nenciu, and T. G. Pedersen, J. Math. Phys. **47**, 013511 (2006).
[25]H. D. Cornean and G. Nenciu, J. Funct. Anal. **257**, 2024 (2009).
[26]D. V. Khveshchenko, Phys. Rev. Lett. **87**, 206401 (2001).
[27]V. P. Gusynin, V. A. Miransky, S. G. Sharapov, and I. A. Shovkovy, Phys. Rev. B **74**, 195429 (2006).
[28]V. P. Gusynin, S. G. Sharapov, and J. P. Carbotte, J. Phys.: Condens. Matter **19**, 026222 (2007).
[29]T. G. Pedersen, A.-P. Jauho, and K. Pedersen, Phys. Rev. B **79**, 113406 (2009).
[30]R. Petersen, T. G. Pedersen, and A.-P. Jauho, ACS Nano **5**, 523 (2011).